RESEARCH REPOSITORY

Amri, A., Jiang, Z-T, Pryor, T., Yin, C-Y and Djordjevic, S. (2014) Developments in the synthesis of flat plate solar selective absorber materials via sol–gel methods: A review. Renewable and Sustainable Energy Reviews, 36 . pp. 316-328.
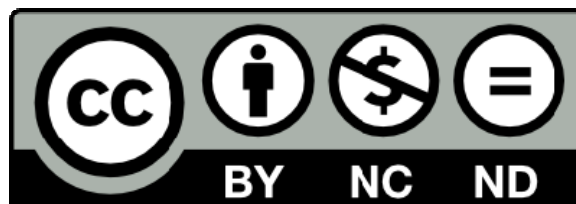
Developments in the synthesis of flat plate solar selective absorber materials via sol–gel methods: A review

Amun Amri[a,b], Zhong Tao Jiang[b], Trevor Pryor[b], Chun-Yang Yin[b,c], Sinisa Djordjevic[b]

[a]Department of Chemical Engineering, University of Riau, Pekanbaru, Indonesia

[b]School of Engineering and Energy, Murdoch University, Murdoch 6150 WA, Australia

[c]School of Science and Engineering, Teesside University, Borough Road, Middlesbrough TS1 3BA, United Kingdom

Abstract

There is a great demand for low-cost and environmentally friendly techniques for synthesizing high quality solar selective absorber (SSA) coatings. Such coatings are capable of absorbing most of the incoming solar radiation (high absorptance) without losing much of the thermal energy through re-radiation from heated surface (low emittance). Sol–gel techniques are promising synthesis methods for these SSA coatings. The optical properties and durability of the SSA coating can be easily controlled by fine-tuning relevant design parameters such as heating temperature or precursor concentrations in the synthesis process. In light of this, there are many knowledge gaps that need to be filled in the context of technicalities regarding the sol–gel processes and the optical and morphological characteristics of these coatings. Comprehensive understanding of these characteristics is a vital component in the optimal design of SSA coatings and therefore, the aim of this paper is to identify these technical issues and review developments in the synthesis of flat-plate SSA materials produced by sol–gel methods.

Keywords: Flat-plate; Solar selective absorber; Sol–gel; Solar energy

1. Introduction

The sun is an unlimited and environmentally friendly source of energy. Solar radiation can be transformed into usable forms of energy such as electricity or heat. Photovoltaic (PV) devices can be used for converting solar irradiation to electricity while solar thermal collectors can convert solar irradiation to the heat which powers a steam generator, i.e. solar thermal power, or for domestic applications [1–4]. One type of solar thermal collector is the flat-plate solar thermal collector usually used for water or air heating at low temperatures (< 150 °C) [5–7]. The key component of a flat plate solar thermal collector is the solar absorber surface, the properties of which strongly affect the efficiency of the solar thermal conversion system. Ideally such surfaces absorb most of the incoming solar radiations (high absorptance) without losing much of the thermal energy through re-radiation from heated surface (low emittance). However, no single material in nature can meet these criteria. As such, there is a need to optimize the optical and structural properties of a surface through the use of a combination of materials, the modification of the surface, or the synthesis of multilayer solar absorber materials to achieve the desired wavelength selectivity [8,9]. Such surfaces are called solar selective absorber (SSA) surfaces.

Generally, SSA materials are categorized as materials with good optical performance if they have absorptance values (α) greater than 90% in the solar wavelength range (0.3–2.5 µm) and thermal emittance values (ε) less than 10% in the mid/far-infrared wavelength ranges (>2.5 µm) [10–12]. However, to be commercially competitive, they should possess α greater than 94% and ε less than 4%. For solar thermal energy, the efficiency of the photothermal energy conversion could be enhanced by the development of new selective absorber materials [13]. Other factors for consideration in the production of photothermal absorbers are long thermal durability, simplicity, cost-effectiveness in fabrication as well as minimal environmental impact in the production process.

Since the mid-1950s, when Tabor [14–16] proposed and established the effectiveness of selective surfaces for increasing the photothermal efficiency of solar collectors, numerous types of solar absorbers have been reported [6]. Electroplating/electrochemical deposition (including chemical

conversion/chemical bath deposition (CBD)) [17–20], vacuum deposition (physical vapor deposition (PVD)/sputtering) [8,21,22], chemical vapor deposition (CVD) [8,23], mechanical grinding [11], and sol–gel methods [24–26] are some of the methods that have been used to synthesize the absorber coatings, but only a handful of these have been applied on an industrial scale [27].

The most widely used industrial solar selective absorbers nowadays are metal particles in ceramic (cermet) structures which are produced by electrochemical or vacuum deposition methods. Some well-known examples include electroplated black chrome ($Cr–Cr_2O_3$) and nickel-pigmented anodic Al_2O_3 (synthesized via the electroplating/electrochemical method) as well as evaporated titanium nitride film ($TiNO_x$) and nickel–nickel oxide ($Ni–NiO_x$) (synthesized via a vacuum deposition/sputtering method) [9,22,28–33].

Although a substantial proportion of flat plate solar hot water collectors have been synthesized using these methods, they still have disadvantages. The electrochemical treatment methods are relatively simple and have a low operating temperature, yet these methods utilize large amounts of material and are not environmentally friendly [11,34,35]. Vacuum and sputtering deposition methods are low in material consumption, have good reproducibility and low levels of environmental pollution but they are, nonetheless, less cost-effective because they require a large investment in rather complicated production equipment with high operational cost and high energy intensity in production [8,10,11,27,34–38]. Other methods of SSA production such as CVD and mechanical grinding also have their plus points and drawbacks. In general, the CVD method has good potential in industrial-scale production but there are difficulties in ensuring the stoichiometry of the metal oxides produced [39]. Mechanical grinding is a simple and cost-effective method of SSA production but the selectivity of the absorber material is low [11,40].

Recent developments in the synthesis of SSA highlight are the creation of a material which has high selectivity and durability and requires a cost-effective and environmentally friendly synthesis process. In this context, sol–gel techniques meet these criteria and they are potentially very promising techniques [28,41–43]. However, the application of these techniques to produce SSA materials is much less common than electrochemical or vacuum-based techniques. The sol–gel methods are well-

known simple, low cost, and environmentally friendly thin film fabrication techniques resulting in a uniform chemical thin film composition [26,44]. The sol–gel processes are a soft chemistry technique where the precursors are generally in the form of a colloidal-based solution that eventually 'transforms' into an widespread network of either discrete or continuously linked molecules. Sol–gel techniques facilitate control of coating parameters such as absorber particle size, particle size distribution, homogeneity, chemical composition and film thickness. The techniques also show good potential for scaling up to an industrial scale [42,45]. The synthesis processes are low in material consumption and can be manufactured under ambient pressure [25,46]. It had been proved that the sol–gel method was able to reduce production costs drastically for absorber thin film fabrication compared to the sputtering method, because the cost for the coating itself could be neglected compared to the substrate cost and that at least half of the raw material costs could be reduced [26]. In terms of energy application, the sol–gel processes do not need the vacuum condition. It is widely known that the vacuum condition preparation needs an advanced and expensive system and needs much higher energy intensity application to generate the vacuum condition compared to the normal calcination processes. Thus, the sol–gel process is low-cost and efficient in energy consumption and much easier to prepare using normal calcination process compared to the vacuum process. The most significant advantage of sol–gel over other established coating methods is its ability to tailor the microstructure of the deposited film [47] at low temperatures.

This paper reviews the developments in the synthesis of flat-plate SSA materials produced by sol–gel methods. To provide a more focused discussion, paint selective coatings have been excluded from this review as they generally have an inferior spectral selectivity [33,48,49] due to the strong absorption by the organic polymer paint binder in the IR range that increases emittance [33,49,50]. Hopefully, this review can provide a platform for material scientists/engineers to intensify their research on the development of cost-effective and environmentally friendly coatings for solar thermal energy applications. By intensifying research on sol–gel processes, it is hoped that the products can compete or even improve on products obtained from electrochemical or vacuum methods. This favorable outcome of this augurs well in regard to advocacy of green and low-cost energy policies especially for

poor and developing countries. After a more detailed consideration of the sol–gel synthesis process, and the solar absorptance and thermal emittance parameters, a detailed discussion of the three major categories of sol–gel synthesis options is provided.

2. Sol–gel synthesis process

The regular sol–gel steps in synthesizing SSA surfaces generally consist of substrate surface cleaning, sol solution preparation, film deposition and heat treatment/calcination. In the solution preparation step, Brinker et al. [47] briefly explained that the sol–gel process involved the use of solid inorganic or metal organic compounds as precursors in a solvent forming a colloidal dispersion. For more detail, in aqueous or organic solvents, these precursors were hydrolyzed and condensed to form inorganic polymers (network) composed of oxo (M–O–M) or hydroxo (M–OH–M) bonds. As for inorganic compounds, hydrolysis proceeded by the elimination of a proton from an aquo ion $[MO_NH_{2N}]^{z+}$ to form an hydroxo (M–OH) or oxo (M=O) ligand (M=metal). Condensation reactions concerning the hydroxo ligands resulted in inorganic polymers whereby metal centers were linked by oxygens or hydroxyls [47]. Any precursors, which form in an inorganic network, can subsequently be utilized in the sol–gel technique. The most frequently used metal organic compounds were metal alkoxides $M(OR)_z$, where R was an alkyl group C_xH_{2x+1}[43]. Generally, the alkoxide was dissolved in alcohol and hydrolyzed by the addition of water within acidic, neutral, or basic conditions. Hydrolysis resulted in the substitution of an alkoxide with a hydroxyl ligand [47]:

$$(M(OR)_z + H_2O \rightarrow M(OR)_{z-1}OH + ROH \tag{1}$$

In essence, the preparation of a sol–gel solution involves the use of inorganic or metal organic compound aqueous organic/alcoholic solvent with the addition of an acid/base conditioner as a catalyst [47]. In this review, any modifications in the solution preparation method as elucidated earlier, such as the addition of a complexing agent, the addition of metal oxide powder or the addition of other additives, as well as the solution preparation without the addition of a catalyst (sol–gel-like) are also classified as sol–gel methods.

In terms of fabrication techniques, there are several deposition options such as dip-, spin-, flow-, spray- and roll-coating which can be used to coat a surface with a sol solution. However, only flow-, spray- and roll-coatings are more industrially viable [51]. Using these various deposition options, it is possible to synthesize different materials in various forms: monoliths, powders, fibers or thin films. As the precursors are mixed at the commencement of the synthesis, the temperatures are generally lower compared to equivalent solid-state synthesis methods such as the mentioned earlier. Furthermore, by utilizing the sol–gel technique, it is possible to synthesize multi-component films with a complex structure [33].

3. Solar absorptance and thermal emittance

An efficient SSA marked by low thermal emittance and high solar absorptance is a feasible concept. The solar spectral irradiance and the thermal infrared spectrum of heated bodies do not overlap to any substantial extent. The terrestrial solar spectral irradiance distribution curve commences at wavelength $\lambda \geq 0.3$ µm, while for $\lambda \geq 2$ µm it is almost insignificant. For temperatures lower than 773 K, most thermal radiation (98%) occurs at $\lambda \geq 2$ µm due to black body radiation [52]. This leads to the following formal definitions.

Solar absorptance (α) is broadly defined as a weighted fraction between absorbed radiation and incoming solar radiation (I_{sol}), while thermal emittance (ε) is defined as a weighted fraction between the emitted radiation and the Planck black body distribution (I_p), and both can be determined in terms of the surface reflectance ($R(\lambda)$) using the following equations [26,53]:

$$\alpha = \int_{0.3}^{2.5} I_{sol}(\lambda)(1 - R(\lambda))\, d\lambda \Big/ \int_{0.3}^{2.5} I_{sol}(\lambda)\, d\lambda \tag{2}$$

$$\varepsilon_{(T)} = \int_{2.5}^{20} I_p(\lambda)(1 - R(\lambda))\, d\lambda \Big/ \int_{2.5}^{20} I_p(\lambda)\, d\lambda \tag{3}$$

Absorptance and emittance of a SSA material are a result of various mechanisms, which depend on the chemical composition and structure of the material. The absorption, transmission and reflection

phenomena in the absorber material can also be determined by physical effects such as intrinsic properties of the material, interference in a double layer (absorber-substrate), interference effects due to interchanging dielectrics and metals, geometrical trapping by surface roughness, and the size effect of metal particles in insulating matrix [6,52]. One of the most common strategies in preparing a spectrally selective surface is to apply a highly solar absorptive thin film onto a non-selective highly reflective metal substrate (absorber–reflector tandem). The absorptive layers need to be transparent in the infrared region to maintain the low thermal emittance of the substrate [45,52,54]. To further supplement the understanding of these concepts, the absorption, transmission and emission in the solar selective absorber–reflector tandem system are illustrated in Fig. 1. The spectral characteristic of an ideal and real selective solar absorber compared with the sun spectrum at AM1.5 and the blackbody-like emission spectra is shown in Fig. 2. The standard spectral solar flux incident at the surface of the Earth, after atmospheric absorption, is limited to the range between 0.3 and 2.5 μm (ISO 9845-1, 1992) i.e. UV/vis/NIR wavelength ranges with the maximum solar intensity at around 0.55 μm, whereas the optical properties of a real body in the infrared wavelength range can be characterized by its thermal emission compared to the ideal blackbody at 100, 200 and 300 °C. Basically, there is no significant overlap between the solar radiation confined in wavelength ranges from 0.3 to 2.5 μm and the emitted thermal radiation in wavelengths above 2 μm especially for temperatures below 200 °C. If the temperature of the blackbody increases, the amount of the emitted energy also increases, and the location of peak power density shifts towards shorter wavelengths. For temperature at around 100 °C the critical wavelengths for the low to high reflectance is about 3 μm while for temperature at around 300 °C the critical wavelength is about 2 μm. These profiles suggest a possibility of designing a thin film material which absorbs the maximum amount of incident solar radiation, and re-emits a minimum amount of the absorbed energy (solar selective absorber surface) that approaches an ideal selective absorber.

In practice, absorptance and emittance are usually measured in terms of reflectivity using UV–vis–NIR and IR instruments, respectively. Table 1 summarizes some of the SSA materials that have been developed using sol–gel methods and the equipment that has been used to measure the absorptance

(α) and emittance (ε) values. It shows that there is no universally agreed set of testing conditions (e.g. prescribed values of air mass or wavelength measurement ranges) for the measurement of the properties of sol–gel SSA materials developed for SSA applications.

The optical characteristic of absorbers is also affected by thin film thickness, surface roughness and the optical constants of the material. Computer simulations have examined the simplest design for composite SSA coatings [55]. This work shows that a high solar absorption can be achieved when the coating has a non-uniform composition with the highest refractive index most similar to the metal substrate and then steadily decreasing towards the interface. Detrimental interference produced in the visible spectrum, by appropriate choice of film thickness, increases the solar absorption up to 98% [55].

The solar absorber layer material may be a transition metal oxide, metal oxide alloy, spinels, or metal/carbon particles in a matrix of either porous or non-porous material. A rough surface and a porous absorber film are normally desirable whereby a rough surface will reduce the amount of reflection of the incident radiation while porosity of materials contributes to the lower refractive index [46,56]. In this way, the absorptance is typically boosted due to the interaction and relaxation mechanism in the absorber and several reflections and resonant scattering in the pores of absorber film [57]. However, in terms of durability, the bare porous absorber films are normally vulnerable and need an impervious and/or dense top most layer to protect it against corrosion. The reflectivity of the underlying metal plays a substantial role in the selectivity of the coatings. For substrate materials, aluminum or copper is normally selected because these metals exhibit good reflective properties in the infrared spectral region (and hence low thermal emittance), high thermal conductivity, and good corrosion resistance [18,33]. Aluminum is the most widely used substrate for low-temperature solar selective absorber applications [58] since it is a relatively light and inexpensive metal [18].

The thickness of the film also influences the selectivity of solar absorber. The optimum thickness should be a compromise between the low thermal emittance and the high solar absorptance. The increase of solar absorptance rendered by a denser coating unfortunately produces a strong increase of thermal emittance, and so the maximum selectivity of a solar selective material is achieved by

optimized layer thickness due to thin film interference. The most usual way to determine this thickness experimentally involves judicious assessment of solar absorptance and thermal emittance for varying thicknesses of samples [52].

4. Metal oxide based selective absorber

Metal oxide, either standalone or blended with other compounds, can be simply synthesized using sol–gel methods. Generally, the synthesis route is relatively short and without the requirement for inert conditions in the calcination step (the heating step following the coating step). This is the reason why research on this subject is relatively extensive. A review of the synthesis and development of this type of SSA material is presented below.

4.1. Copper oxide-based absorber

Copper oxide (CuO), which is well-known for having good optical properties as SSA material, is inexpensive and easy to process using sol–gel methods [59]. The other principal oxide of copper, Cu_2O, also exhibits good solar absorption, but its absorption is lower than CuO [60]. Hottel and Unger [61] prepared bare CuO as an SSA coating on flat-plate collectors. Coating deposition was carried out by spraying a dilute solution of cupric nitrate onto an aluminum sheet, which converted the cupric nitrate to black cupric oxide by heating it to above 170 °C. This oxide film had α=0.93 and ε=0.11 at 80 °C. This selectivity value is comparable to that obtained from various methods such as sputtering (α=0.75, ε=0.1) [60,62], CVD (α=0.73–0.9, ε=0.04–0.52) [23,62], electrochemical (α=0.94, ε=0.08) [20] and combination methods (thermal, chemical and electrochemical) (α=0.97, ε=0.2) [63]. However, the bare copper oxide experienced significant absorptance degradation after exposure to higher temperatures (above 150 °C) in air. This was associated with a chemical structure change [63] and a decrease in the surface roughness of the coatings by heat [6,64]. This has hindered more extensive application, and so further modification is required to improve its durability.

Efforts to protect the bare CuO absorber have been made by many researchers using various methods as summarized by Sathiaraj [65]. Barrera et al. [59] overcame the problems associated with bare CuO by protecting it in a silica matrix forming a CuO–SiO$_2$ composite absorber using a sol–gel process. Silica was selected as the matrix due to its stable oxide state, ease of manufacturability and cost-effectiveness. The sol was prepared by mixing Cu-propionate solution in a TEOS (tetraethoxysilane/tetraethyl orthosilicate) solution and subsequently adding HCl. Film deposition was accomplished by dip-coating on stainless steel substrates. The final film was then annealed in air at 450 °C for 4 h [59]. Barrera-Calva et al. [59]suggested that throughout the annealing process, copper-propionate complexes developed into polycrystalline CuO dispersed in a partially crystallized silica matrix. The thermal analysis of gel showed that the synthesized material may be stable up to 400 °C. The solar parameters of such a system were strongly influenced by the thickness and phase composition of the CuO–SiO$_2$ film. The optimized solar parameters (α=0.92, ε=0.2) were exhibited for the thinnest films (one dipping cycle) which consisted a CuO–Cu$_2$O mixture embedded in a partially crystallized silica matrix [59]. However, the relative high emittance values in this research could be due to the strong silica phonon absorptions [50].

One way used to attain maximum solar absorption and reduce thermal emittance is to synthesize an optimized porous antireflection (AR) layer or matrix with an optimized surface roughness as suggested by Farooq and Lee [55]. The porosity decreases the refractive index of the AR layer or matrix in which refractive index can be optimized via tuning (i.e. square root of the refractive index of the underlying material), whereas the increase in the roughness of the film up to 1×10^{-7} m rms (root mean square) increases the absorption proportionally. Any further increase of roughness raises the thermal emittance because of the thermal radiation absorption [55].

4.2. Cobalt oxide-based absorber

Besides copper oxide, cobalt oxides (CoO or Co$_3$O$_4$) also have good optical properties as SSAs and are comparatively easy to synthesize. The idea of using cobalt oxide as a selective absorber material was first introduced by Gillette [56,66]. In terms of sol–gel techniques, many researchers are more interested in the synthesis of cobalt oxide than copper oxide. This is attributed to the fact that cobalt

oxide is more stable at high temperatures than copper oxide. For example, two types of cobalt oxides, namely Co_3O_4 and CoO, are stable at temperatures above 500 °C [56,67,68]. However, cobalt oxide precursors are relatively more expensive than the copper oxide precursors but this cost is still negligible compared to the substrate cost.

Choudhury et al. [69] synthesized a black cobalt selective surface via spray pyrolysis on top of aluminum and galvanized iron substrates. They found that the film had a relatively good selectivity. Optimized films on aluminum substrate (about 0.21 μm thick) had α=0.92 and $\varepsilon_{100\ °C}$ =0.13 while films on galvanized iron substrate (film thickness=0.24 μm) had α=0.91 and $\varepsilon_{100\ °C}$=0.12. Accelerated ageing studies indicated that these films had excellent adhesion to the substrates. Nonetheless, the films were only stable up to 220 °C and there was degradation at higher temperatures [69,70].

In a separate study, Chidambaram et al. [71] prepared cobalt oxide coatings by spray pyrolysis on stainless steel substrates at 300 °C. The coatings adhered sturdily on the substrate and were stable up to 600 °C. Auger electron spectroscopy, X-ray photoelectron spectroscopy and X-ray diffraction investigations showed that the coatings consisted of an upper layer of Co_3O_4 with a CoO layer near to the substrate. The integrated solar absorptance value α was 0.93 and hemispherical emittance value ε (at 100 °C) was 0.14. However, heat treatment for several hours at 600 °C altered these absorptance and emittance values to 0.89 and 0.19, respectively [56].

Chidambaram et al. [71] indicated that a lower substrate temperature of ca. 150 °C could be utilized for the preparation of coatings if an equimolar aqueous solution of cobaltous acetate and thiourea was used. These coatings contained cobalt oxide and cobalt sulfide and exhibited somewhat similar absorptance values but they had higher emittance values. The addition of cobalt sulfide rendered lower quality of the sulfured film and it became worse after thermal annealing [72]. These coatings were stable only up to about 250–300 °C [54,71]. Additional work is required to develop the coating quality using this method. Barrera et al. [73] suggested the use of stainless steel containing', or copper, as a substrate.

Uma et al. [54] expected that if another stable oxide (like iron oxide) was added to the cobalt oxide precursor solution system then higher stability and optical performance could be achieved because the cobalt oxide–iron oxide coating was found to be stable up to 300 °C. Iron oxide exhibits lower refractive index than cobalt oxide and hence the combination increased absorptance. They synthesized a cobalt oxide–iron oxide (CoFeO) solar selective coating on stainless steel using a spray pyrolysis technique and found that the coating had an absorptance of $\alpha=0.94$ and an emittance of $\varepsilon_{100}=0.20$. It was found that the coating had high mechanical stability for temperatures up to 400 °C.

Avila et al. [72] synthesized cobalt oxide thin films on stainless steel and nickel–stainless steel alloy using a spray pyrolisis technique at temperatures of 350–600 °C during a 5-h period. Cobalt nitrate dissolved in water–ethanol was used as the precursor. The absorptance value of $\alpha=0.77$ and the emittance value of $\varepsilon=0.20$ were achieved when the stainless steel substrate was used. Interaction between the stainless steel substrate and the coating material was also detected as evidenced by the presence of an iron austenite phase. Greater thickness and roughness of the Co_3O_4 film also contributed to a better absorptance. This phenomenon was consistent with the research results obtained by Drasovean et al. [74] for wavelengths between 300 and 800 nm. However the greater thickness of Co_3O_4 also had negative effect, increasing the thermal emittance. Other efforts to improve selectivity were focused on changing the other experimental conditions. The higher the annealing temperature, the higher the film roughness would be [72].

Efforts to improve the quality of the cobalt oxide selective absorber surface by using simpler deposition techniques such as dip-coating have also been made. Cathro [56] outlined that spray pyrolysis should be avoided because there were mechanical difficulties in controlling the accuracy of the film thickness [75]. Cathro prepared SSA surfaces based on cobalt oxide, either standalone or in an admixture with nickel/manganese oxide via a sol–gel dip-coating process. In the process, mild steel substrate was immersed in the ethanolic cobalt nitrate solution and withdrawn at 10 mm/s before being pyrolized at 500 °C for 15 min. The addition of nickel nitrate to the cobalt oxide solution precursor increased both absorptance and emittance of the final film, whereas the integration of manganese decreased emittance. Addition of a deposit containing 5% nickel afforded solar

absorptance of 0.90 with thermal emittance ranging from $\varepsilon=0.1$ at 80 °C to $\varepsilon=0.25$ at 300 °C. In other conditions, addition of colloidal silica improved the optical properties of the film. In terms of mechanical properties, these surfaces were stable for at least 1000 h at 500 °C [56]. Barrera et al. [67] reported that black cobalt (Co_3O_4) thin film made by sol–gel dip coating onto a stainless steel substrate showed $\alpha=0.88$ and $\varepsilon=0.12$. Cobalt acetate was used as the precursor and it would become a gel in a few hours. Cobalt acetate was obtained from precipitation of $CoCl_2$ aqueous solution by ammonia, and then it was dissolved in acetic acid to form a cobalt acetate solution precursor. During the dipping process, the relative humidity was maintained at 40% in the preparation chamber and the dipping speed was 1 mm/s. The coating colors depended on the thickness of the films. A film thickness of around 0.08–0.25 μm could be obtained depending on the viscosity of the precursor. Less viscous sols (<2 cp) produced a film thickness of 0.08 μm/dipping while for relatively more viscous sols, the film thickness increased to 0.25 μm/dipping. The durability test showed that the coating had good stability at high temperatures of 450 °C for 48 h. However, the multiple repetitions of the coating using a fix speed rate of dip-coating had a weakness, namely it created many defects which influenced the mechanical and optical characteristics of the films [37]. As a comparison, the electrochemical method used to synthesize a cobalt oxide selective absorber on various substrates gives $\alpha=0.92$–0.96 and $\varepsilon=0.04$–0.18 [76–78]. Overall, it can be concluded that the cobalt oxide selective absorber produced by the sol–gel dip-coating method is quite comparable with the electrochemical-based cobalt oxide selective absorber.

To avoid the degradation performance of the absorber material, the protecting layer is required to cover the bare cobalt oxide absorber layer. Barrera et al. [25] synthesized the cobalt oxide in a silicon matrix forming amorphous cobalt–silicon oxide thin film on the stainless steel substrate using a sol–gel dip coating route. Cobalt (II) acetate tetrahydrate and tetraethyl orthosilicate (TEOS) were dissolved into the acidified ethanol. Concentrated HCl was also added dropwise and then the solution was stirred for 24 h at room temperature. The Co(II) ion in the sol was stable based on the FTIR experimental results. There was Co(II) chelation between OAc^- ion from HOAc with Co(II) stabilizing the Co and avoiding precipitation. This solution was also used for the dipping procedure.

After the dipping process, all samples were heat-treated at 400 °C so that the gels adhere to the substrates. The absorptance value of the thin film is not high (α=0.82) but it showed high thermal stability. The role of the silica matrix was to protect the cobalt oxide from performance degradation. The sol–gel process was an appropriate technique for synthesis of a homogeneous thin film; in this case, cobalt was incorporated homogeneously into the silica matrix. FTIR detected the Co–O–Si bonds in the film, which indicated that homogeneity extended to the molecular scale [25]. Unfortunately, the silica matrix absorbed too much EM radiation in the IR wavelengths (around 8–10 µm) producing an increase in the emittance and a decrease in selectivity [50,79].

Barrera et al. [44] also used tin oxide (SnO) as a protecting layer for black cobalt. Tin oxide was chosen because of its low emissivity [79–81] and high chemical stability [82]. Black cobalt and tin oxide were deposited by the sol–gel dip-coating method onto the various substrates. Cobalt-propionate solution was used as the cobalt oxide precursor, while a peptized tin carbonate aqueous solution was used as the tin oxide precursor. They found that the use of glass and stainless steel substrates improved selectivity slightly, while the use of a nickel stainless steel substrate, even though it only gave a moderate absorptance value, decreased emittance values significantly where α=0.72 and ε (at 100 °C)=0.037 [44]. Besides Co_3O_4, the Co_2O_3 compound also existed in the films. Large amounts of carbon as graphite particles and carbides were also detected in several configurations. In a ---tin oxide protecting layer, SnO_2 phases and carbon particles were also detected. The presence of carbon was caused by the relative low annealing temperature (400 °C) [44].

Barrera et al. [83] also tried a different approach to obtain a durable SSA by mixing cobalt and copper oxide precursors without adding a protecting layer. They prepared polycrystalline cobalt–copper oxide alloy (CoCuO) thin films on stainless steel (SS) substrates using the spray pyrolysis method. This preparation was simple and required low consumption of reagents. A mixture of cobalt and copper nitrate with the molar ratio of Co:Cu (5:1) in ethanol:water (3:1) solvent was used as the precursor solution. After 3 min spraying deposition, the samples were heated to 300–600 °C for 3 h. The films were stable up to 400 °C and showed good absorptance (α=0.84) but the emittance was also relatively high (ε=0.28) reducing the performance of selective absorber. A complex chemical structure

consisting of Co_3O_4, CuO and metallic copper phases, as well as voids was detected by X-ray diffraction and ellipsometry studies.

4.3. Ruthenium oxide

Morales-Ortiz et al. [84] found that a ruthenium oxide (RuO_2) thin film on the top of an ASTM grade 2 titanium substrate produced the characteristics of a SSA. Ruthenium chloride in alcoholic solution was used as a precursor solution. The deposition was carried out using the dipping and spraying technique at room temperature before the sample was heat-treated at a temperature of 450–500 °C for 1 h. In the case of dipping a polished substrate, the absorptance was 0.74 while the emittance was 0.12. For spray deposition onto a non-polished substrate, the film exhibited a very high solar absorptance (α=0.98), but unfortunately also a very high infrared emittance (ε=0.8). Therefore to improve performance, a thin gold film was added to the surface of the ruthenium oxide by evaporation giving an absorptance value of 0.91 and an emittance value of 0.16. The close control of the deposition parameters and the substrate surface roughness would allow further improvement in selectivity and reproducibility.

4.4. Metal oxides composite blend

A film consisting of nickel oxide (NiO) in the pores of alumina ($NiO–Al_2O_3$) on an aluminum substrate also showed the characteristics of a SSA material. Ienei et al. [12] prepared NiO films obtained by sol–gel spray pyrolysis deposition (SPD) using an aqueous solution of nickel acetate tetrahydrate embedded in a porous structure of Al/Al_2O_3. They optimized the precursors' concentrations and compositions, substrate temperatures and annealing treatments to produce the best SSA. The coatings had good spectral selective characteristics with a solar absorptance of 0.92 and a thermal emittance of 0.03. A low thermal emittance value was obtained after using hydrophobic polymer additives (sodium maleat-methyl metacrylate (HFB)) and annealing treatment. The films' solar absorptance and thermal emittance were correlated to their chemical composition, crystallinity and morphology. In terms of layer-by-layer deposition (e.g. substrate–selective surface–antireflection (AR) layer), a high surface energy (low contact angles) of the intermediate layer (absorber layer) was

recommended to allow the deposition of the next layer from aqueous/polar precursors. The surface of the last deposited layer should have large contact angles, and thus low surface energy. This would ensure non-wetability and therefore a cleaner surface which would prevent condensation of any water vapor that might enter into the collector onto the surface of the thin films [12].

Another sol–gel route to synthesize a NiO–Al$_2$O$_3$ SSA film was reported by Qian et al. [85]. They used an aluminum isopropoxide and nickel nitrate solution and deposited it onto a stainless steel substrate by dip-coating. The results showed that a compact and homogeneous film was obtained when the withdrawal speed was 1 mm/s, the NiO content in the sol was 20% and the thermal treatment temperature was 700 °C. The addition of a silica antireflection layer on the uppermost absorbing layer could enhance the effectiveness of the absorber. The optimal performance of an antireflection coated sample could reach a solar absorptance of 0.84 [85].

Dudita [86] has synthesized the copper oxide–nickel oxide composite selective absorber on a copper substrate by the robotic spray pyrolysis method at 330 °C. The solutions used were a mixture of nickel acetate and copper acetate in water–ethanol solution based on the previously optimized conditions [87]. The best selectivity (36.4) was obtained from film with highest roughness (precursors with 40% ethanol). They proposed two parallel mechanisms of high selectivity: intrinsic absorption and multiple reflections generated when absorbers with controlled roughness are deposited [86].

5. Metal and carbon particles in dielectric matrix

5.1. Incorporation of metal particles in dielectric matrix

Certain metallic clusters embedded in a ceramic/dielectric matrix (cermet) such as Cr–Cr$_2$O$_3$, Mo–Al$_2$O$_3$, or Ni–NiO$_x$ exhibit good solar spectral selective absorption. The metal particles in the cermet act as a modifier for the optical response of the ceramic phase [50,88]. The absorption in a cermet coating is a result of light scattering by the boundaries between the metallic phase and the oxide

(dielectric) phase [89,90]. Generally, the spectral selectivity of a cermet coating is enhanced by using a poor thermal emitter metal substrate [46,91].

The concept of using a cermet material to form a tandem structure with a poor thermal emitter metal substrate has been examined [22,55]. Cermet selective absorbers typically comprised of nanometer-sized metal particles (1–20 nm) [92] and the effective medium theories can be utilized to model the optical characteristics of the film [93,94]. Simulations have proved that a ceramic–metal solar absorber with AR layer could achieve absorptance values of 0.91–0.97 and emittance values of 0.02–0.07 [92].

The cermet system affords a high degree of flexibility which the optical parameters can be tuned by controlling the metal content, shape, size and orientation of small metallic clusters. The thickness and chemical nature of the dielectric phase can be adjusted to obtain the desired spectral selectivity. The type of matrix also influences the quality of the film. In this regard, a porous matrix is the optimum host for metal particle inclusion [6,26,46,91,95]. The surface morphology of cermet also plays a significant role in determining the surface absorptance and can favor multiple reflections in the surface, thus enhancing the solar radiation absorption [12]. By varying many parameters listed earlier, countless combinations can be produced. Thus, the required spectral selectivity can be effortlessly attained [26].

Many researchers in the field of SSA synthesis have investigated cermet selective absorbers using various synthesis methods. This is because the cermet structure is unique and it is one of the highest performance selective surfaces [95]. However, to the best of our knowledge, the synthesis of this type of absorber using sol–gel methods is relatively scarce. Eisenhammer et al. [96] patented the idea of metal/conductive particles in alumina, with either $Al_{65}Cu_{20}Ru_{15}$ in alumina or TiN in alumina, as a SSA. Each composite was obtained by mixing the conductive particles with an alumina matrix sol precursor. The alumina sol precursor was prepared by dissolving niobium chloride ($NbCl_5$) in butanol and mixing with sodium butoxide ($Na(OBu)_n$) under reflux conditions. This produced $Nb(OBu_n)_5$ which was subsequently mixed with glacial acetic acid to form the alumina sol precursor. They also investigated another route to prepare the alumina sol precursor by mixing boehmite with

HNO_3 at 55 °C. For the synthesis of quasicrystal $Al_{65}Cu_{20}Ru_{15}$ conductive particles in alumina film, the particles were mixed with the alumina sol precursor solution which was then sprayed onto a copper substrate and heat-treated at 600 °C. For synthesis of TiN conductive particles in alumina film, the particles were dispersed into the alumina sol precursor solution and then coated on the copper substrate by centrifugation (spin) and finally heat-treated at 600 °C. The $Al_{65}Cu_{20}Ru_{15}$ alumina layer had a thickness of 110 nm and a volume fraction of 30%, whereas the TiN–alumina layer had a thickness of 130 nm and a volume fraction of 20% [96]. However they did not show any absorptance and emittance values, but from the curves created in their patent, these two SSAs can be categorized as having comparable selectivity values.

Bostrom and co-researchers [26,41,43,51,91,97–99] have synthesized nickel nanoparticles embedded in an alumina ceramic matrix ($Ni–Al_2O_3$) thin film on a smooth and highly specular aluminum substrate using a sol–gel-like method. They reported that although the sol–gel techniques have been known to synthesize a wide range of materials for many decades, it was only recently that solution-chemistry science was found to be an appropriate technique to synthesize nanoparticle composites which are suited for thermal solar absorber applications [24,26]. Precursor solutions of nickel and pure amorphous Al_2O_3 in different proportions were mixed to control the nickel to alumina ratio in the final absorbing films [26]. Film deposition was conducted via spin-coating at 3700 rev/min for 20 s before the film was heat-treated to temperatures of 550–580 °C in an oxygen free glass tube. Subsequent to heat treatment, solvents were evaporated in which only alumina and metallic nickel remained in the final film coating [26,98]. The thin films produced were homogeneous with a nickel content of up to 80% of the volume fraction. They suggested that to construct a more efficient Ni–Al_2O_3 absorber layer, the bottom part of the layer should have high nickel content while at the top it should have minimum nickel content [26]. The use of a rough aluminum surface as a substrate was also implemented in this research, but the results were less satisfactory than the smooth substrate.

Further investigations by Bostrom and co-researchers [51] focused on improving the selectivity and durability of the nickel–alumina cermet and enhancing the performance of the AR coatings. They reported that the performance of the nickel–alumina selective absorber thin film system was improved

if a three-layer system was applied. This film was composed of an 80% nickel and 20% alumina with the thickness of 103 nm at the base (first layer), a 40% nickel–60% alumina film with the thickness of 59 nm in the middle (second layer) and a silica/hybrid-silica film with the thickness of 90 nm at the uppermost layer (third layer/AR layer). This optimal three-layer system exhibited a solar absorptance value of 0.97 and a thermal emittance value of 0.05 [41,43,51,99]. These results were comparable to commercial products. These synthesis processes were simple and cost-effective but the nickel–alumina solution was unstable and agglomerated to form precipitates within 24 h, thus reducing the reproducibility of this system, even though the stability can be enhanced for up to 1 week in a methanol solution [98]. The calcination step also required strictly oxygen free conditions, which was troublesome. This absorber is being industrially produced on a pilot scale since 2009 and the company is working on having a full scale process in the near future.

Another effort to improve the nickel–alumina SSA coatings synthesized using a sol–gel-like method was carried out by Nejati [36]. Nejati used nickel nitrate and alumina powder as precursors. Nickel nitrate was first dissolved in distilled water or ethanol, and then while stirring, alumina powder was gradually added. The prepared mixture was then dispersed mechanically using a dissolver and ultrasonication. To avoid agglomeration, the temperature was strictly controlled and different additives such as a wetting agent; a coupling agent and a dispersing agent were added to the suspension before dispersion. Cleaned aluminum substrates were then dip-coated in the suspension with different speeds. The wet films were dried for 30 min at 120 °C and then quickly annealed for 1 h at 450 °C in a hydrogen atmosphere. Nejati found that the mechanical properties of a pure Ni–Al_2O_3cermet composite layer and the substrate were poor and the layers were easily removed during the tape test. Nejati did not only use TEOS as a source of silica for the AR layer but also used it to enhance the bonding ability between the absorber thin film and the substrate (the silica was also used as an underlayer). Adhesion and scratch resistance of the film was improved significantly. The silica network formed after the addition of TEOS also enhanced the solar absorption by lowering the effective refractive index of the film. However, although the addition of the silica AR layer increased the solar absorptance value, it also increased the emittance value slightly. The best result was shown

by a sample with an absorptance value of α=0.94 and an emittance value of ε=0.11 [36]. Based on accelerated ageing and humidity studies, Nejati estimated that the nickel–alumina absorber was suited for glazed collector applications such as domestic solar water heater operating at low temperatures. Due to the promising optical performance and good thermal and humidity stability, the developed absorber film could compete with sputtered absorber films [36].

Wang [100] demonstrated synthesis of solution-processed plasmonic Ni nanochain–alumina on a stainless steel substrate as the solar selective absorber via sol–gel like method. The Ni nanochains (a diameter of ~80 nm and a length of 2–3 μm) were synthesized by reducing Ni^{2+} with N_2H_4 and they were dispersed in an Al_2O_3 sol for spin-coatings. The final annealing at 400 °C for 1 h in N_2 atmosphere was required to form 1 μm-thick cermet coating. Solar absorptance >90% and thermal emittance <10% were obtained for such coating.

Khamlich [101] synthesized Cr/α-Cr_2O_3 cermet thin film coating on the rough copper substrate via sol–gel like method. Aqueous solution of $Cr(SO_4)_2.12H_2O$ (1 mM) were used as a sol precursor to dip the substrates. The coated substrate was then heated in an oven at a constant temperature of 75 °C. Finally, the coatings were annealed in a flowing H_2 gas at 500 °C for 1 h. Even though a good spectral reflectance was obtained in UV–vis range, no absorptance and reflectance data were reported.

5.2. Carbon particles in dielectric matrices

Katumba et al. [45] outlined the reasons for studying carbon-in-silica tandem selective solar absorbers. Firstly, carbon and silica are relatively ubiquitous, environmentally friendly and highly stable. On the other hand, metallic absorber particles have a tendency to degrade over an extended period due to oxidation. However, if there is a dense AR layer on top of the sol–gel metallic particle layer, this issue is not relevant anymore. Secondly, the relatively minute size of carbon particles (< 10 nm) have a high absorption cross-section in the context of UV–vis radiation [45,102]. Finally, carbon–silica composites could be easily synthesized using sol–gel techniques.

Mastai et al. [57] introduced a new concept for the design of carbon–silica based SSA materials. They showed that porous carbon–silica hybrid nanocomposites have SSA characteristics. The synthesis of

these composites involved a sol–gel-like method to perform a direct carbonization in the nanoconfinements of porous silica leading to the formation of nano-sized amorphous carbon particles. Materials used included sugar as a precursor of carbon, and cyclodextrins (CD) and polystyrene-polyethylene oxide (SE) as precursors of CD-based silica and SE-based silica, respectively. At the end of synthesis process, the binder templates were removed via calcinations in air at temperature ≥550 °C for several hours in a tube oven [57]. In such a structure, solar radiation was absorbed and transferred into heat without infrared re-emission. The carbon nanoparticles contributed to high absorptance and thermal stability, whereas silica contributed a transparent matrix and binder material. Especially in the case of CD-based silica, the overall processes were ideal because of cheap and "green chemistry" conditions. Also, sugar was easily available and non-toxic. This composite was obtained under one-pot synthesis conditions with the elimination of water. No removal or addition of any further chemical was necessary to obtain the non-toxic carbon-containing silica. In addition, leaching of the final material was practically impossible and if that happened it would only release materials that were already abundant in nature [57].

The absorptance and emittance values for the SE-based carbon–silica composite were $\alpha=0.93$ and $\varepsilon=0.08$ respectively, while that for the CD-based silica–carbon composite the absorptance value was 0.92 and emittance value was 0.13. All samples showed excellent stability under humid conditions and high temperatures. Based on the nature of the components involved in this composite, it could be assumed that long-term stability of the samples was likely to be high. The degradation of solar thermal absorber coatings which was usually caused by thermal oxidation of metal particles did not happen in this composite [57].

In separate but related research, Katzen et al. [103] created a carbon–silica nanocomposite film selective absorber on a glass substrate. The film was synthesized using the sol–gel spin-coating method. The silica sol preparation was followed by CD-based silica–carbon composite preparation. β-Methylated cyclodextrin (2 g) was dissolved in 3 g of aqueous HCl and 4 g tetramethylorthosilane (TMOS) was stirred until a homogeneous solution was produced (within a few minutes). The films were spin-coated at 4000 rpm for 1–2 min. The films were then dried and annealed under nitrogen

(95%) flow at 850 K. All films prepared by this method contained approximately 15% carbon. It was found that the best thin film silica–carbon nanocomposite (thickness 1000 nm) showed α=0.94 and ε=0.15. The films showed good mechanical stability under the influence of humidity, as they were held above a water bath at 100 °C for 5 h and in a high temperature environment (250–300 °C) for 48 h [103].

Inspired from Mastai′s [57] research, Charlot [104] used Zirconia to partially or completely substitute the silica matrix to enhance the selectivity of carbon–oxide nanocomposite absorber film coating. The films were fabricated using a sol–gel synthesis of hybrid precursors i.e. tetraethyl orthosilicate (TEOS)+methyl-β-cyclodextrin (MβCD) or colloidal zirconia+MβCD, followed by carbonization in an argon atmosphere at 400–540 °C for 1 h. The optimum selectivity α/ε=32 was achieved in a C/SiO_2 sample deposited onto a copper substrate. The thickness of the films influenced the optical properties of the samples and not by the nature of the deposited layer although this parameter strongly modifies their surface.

Carbon nanoparticles dispersed in ZnO and NiO dielectric matrices on aluminum substrates, to be used as SSAs, have been prepared by Katumba et al. [10]. The sol–gel-like method used to prepare these samples was somewhat similar to the technique proposed by Liu et al. [105] in which zinc acetate dihydrate and nickel acetate tetrahydrate were used as precursors. Efforts to scale up the C/NiO selective absorber have been carried out [106,107]. Titanium dioxide (TiO_2) has also been used as the host for carbon particles for SSA applications. Rincon et al. [46] synthesized carbon blacks (CB) and nanotubes (CNT) integrated in a TiO_2 matrix dispersed on stainless-steel substrates. The coating system was thermo-mechanically stable and free of corrosion problems due to the hydrophobic nature of carbon.

The multiwall carbon nanotubes (MWCNTs) embedded in NiO matrix composite on an aluminum substrate as a solar selective absorber has been synthesized by Roro et al. [108]. The synthesis was carried out via sol–gel process using nickel acetate in ethanol solution, chelating agent, chemically functionalized MWCNTs and a structure directing template. After spin coating, the samples were then heat-treated at 450 °C in nitrogen atmosphere for 1 h. No cracks were observed on the film surface.

The optical performance showed that the coating had an absorptance value of 0.84 (for a single layer) and the thermal emittance of 0.2 (at 100 °C).

Despite many advantages in the use of carbon absorbers in the matrices described above, the optical performance of these absorber materials has not yet reached a satisfactory level. As such, there are still many opportunities for further research to improve their optical properties and durability before commercialization. Besides that, the processes involved are relatively long and cumbersome since in the carbonization process, an inert environment is required.

6. Solar selective absorber surfaces using spinels

6.1. $Cu_xFe_yMn_qO_x$ and CuCoMnO$_x$ spinels

During the last decade, spinels deposited on highly reflective metal substrates have attracted considerable interest due to their promising properties as SSAs for solar thermal collectors. The term spinel refers to a group of minerals which crystallize in a cubic (isometric) crystal structure. Kaluza et al. [50] have succeeded in synthesizing CuFeMnO$_4$ black film spinel SSAs using sol–gel dip-coating and heat-treatment at 500 °C. Mn–acetate, Cu– and Fe–chloride precursors were used in a molar ratio of 3:3:1, respectively. To protect the spinel from corrosion, a 3-aminopropyltriethoxy silane (3-APTES) silica precursor was added to the Cu, Mn and Fe sol precursors with a molar ratio of (Mn–Cu–Fe):silica=1:1. Analytical results showed that the films consisted of two layers: the lower was amorphous SiO$_2$ and the upper was a spinel having the composition of $Cu_{1.4}Mn_{1.6}O_4$. The films exhibited absorptance values of around α=0.6 and emittance values of ε=0.29–0.39.

Hallenstvet et al. [109] patented the manganese copper iron mixed oxide pigment particles with ceria (CeO$_2$) as an inorganic binder via the sol–gel method. The pigment particles and the ceria binder precursor (CeO$_2$ (NO$_3$) with 20% CeO$_2$ having a particle size of 10–20 nm) were mixed followed by application of the mixed sol lacquer on the aluminum substrate and subsequently heated at a maximum temperature of 600 °C forming a manganese ferrite black spinel, $Mn_3Cu_2FeO_8$, solar

selective absorber. The coating exhibited high solar absorptance in UV–vis–NIR area (≥95%) and a thermal emittance of ≤10%. The coating with ceria binder performed well with respect to the adhesion and scratch resistance after heating to 600 °C. However, the reaction in humid air at a required high temperature to obtain the sol–gel coating applied in the synthesis is troublesome.

Some efforts have been taken to improve the optical performance of the manganese copper iron mixed black film spinel oxide. Kaluza et al. [24] reported that the emittance value could be decreased by substituting silica with zirconium oxide (ZrO_2), but of the presence of the ZrO_2 generated a brown hue which caused the absorptance value to drop. A facile method used to synthesize CoCuMn-spinel solar selective absorbers was reported by Bayon et al. [58]. Copper, cobalt and manganese nitrates were mixed in ethanol at different molar ratios in which a complexing agent and a wetting additive were also added to enhance the film adherence. Although the $CoCuMnO_x$ synthesized via this method is often contaminated by some metal oxides, chlorides, and oxychlorides, it is better than the co-precipitation method. This is because in the co-precipitation method, it is difficult to control all the metal cations that precipitate from the solution and which, at the same time, result in composition segregation and low yield [110].

6.2. $CuMnO_x$ spinels and $Cu_xCo_yO_z$ spinel-like

A simpler $CuMnO_x$ spinel which contains less than three metal components and is derived from the CuCoMn-spinel also shows the characteristics of a SSA. Bayon et al. [28] reported that CuMn-spinel thin films on aluminum foil synthesized by a sol–gel-like dip-coating method and followed by air-sintering at 500 °C could be used as a low temperature application of SSA. Since the synthesis process was conducted under the Consortium Agreement of Confidentiality (patent), no detail about solution composition was provided [111].

A solid-state redox reaction occurred when temperatures higher than 450 °C were applied [111]. The highest solar absorptance of α=0.87 is reached by using a one layer film deposited from solutions with a molar ratio Cu/Mn=1. The optical property of the film was dramatically improved by subsequently depositing a SiO_2 anti-reflective layer using a sol–gel technique. By optimizing the thickness of both

CuMn-spinel and SiO_2 layers, the best absorptance and emittance (at 100 °C) values achieved were 94% and 6%, respectively (Fig. 3). Although the optical performance of this spinel oxide solar absorber was quite promising, it was still not sufficiently high to be economically viable. The absorptance of this absorber surface could be improved to 0.95 by integrating a CuMn–oxide absorber layer (a total of three layers) [42]. Thermal stability and humidity tests were conducted based on the method stipulated by the International Energy Agency (IEA) for the Solar Heating and Cooling (SHC) Program Task X for low-temperature SSAs [112,113].

A $Cu_xCo_yO_z$ spinel-like structure on an aluminum substrate has been synthesized via facile sol–gel process for a selective absorber [114]. Copper acetate and cobalt chloride were mixed using absolute ethanol. Propionate acid was subsequently added to the solution as a complexing agent and stirred for 2 h. The resulting solution was used for thin film deposition on aluminum substrates via the dip-coating method. The coatings with distinct thicknesses were synthesized by repeating the dip cycle before final annealing in oven at 500 °C for 1 h in air atmosphere. The absorptance of 83.4% (prior to the addition of an antireflection layer) was accomplished using 0.25 M copper acetate and 0.25 M cobalt chloride (Cu/Co ratio=1) with dip-speed 120 mm/min (four cycles). Nanoindentation test using the Berkovich indenter showed that the coatings have a high wear resistance [115–117].

Overall, based on above explanations, the general strategy to implement sol–gel methods for the synthesis of absorber–reflector tandem structures (non-organic binder) suitable for SSA materials is shown in Fig. 4. For selective absorbers which are prepared without using any easy-to-settle materials in precursors solution (one phase of sol), the route A is proposed as the general route. In this route, atmospheric heat treatment/calcinations are usually applied. If wet film/coating contains high molecular weight organic compounds, the calcinations above 400 °C are needed to ensure no organic compound remains to avoid the mid/far-infrared absorption by the organic compound, and vice versa. While for absorber material which is prepared using easily-settled materials in precursors solution (particles/suspension system sol), route B is suitable. Special treatment is needed to avoid fast precipitation of sol precursors while inert/hydrogen heat treatment at high temperature (>400 °C) is

required to lead the formation of metal/carbon particles in matrix composite. Absorptance, emittance and selectivity of various SSAs produced by sol–gel methods to date are summarized in Table 2.

7. Effect of silica thickness

Various SSAs, whether synthesized by sol–gel or other methods, often involve the incorporation of silica to improve their selectivity or durability. The deposition of a silica layer, especially silica as an AR layer, usually necessitates a sol–gel technique even though the absorber film was deposited by other methods besides sol–gel. In this review, the use of silica (SiO_2) as an antireflection (AR) layer, a matrix or an underlayer has been mentioned, and it also has been discussed elsewhere [118–120]. However, we would like to emphasize here that the use of silica as a protecting agent (matrix or underlayer) of the absorber film has had an unfavorable influence on the optical performance. High emittance values are the consequence of the incorporation of silica as a matrix and/or an underlayer because the silica absorbs too much solar radiation in IR range [24,36,50,59], while silica as an AR layer has a more positive effect because it can improve absorptance with a non-significant influence on the increase of the surface emittance value [28,33,51]. Silica as an AR layer is frequently synthesized thinner than the silica as a matrix or an underlayer, so in the construction of SSA protective layer (matrix or underlayer) involving silica, the protective layer thickness should be an important factor to be optimized. The AR layer or other protective upper coatings should normally be within 50–70 nm or in the scale of tens of nanometers [48].

8. Conclusions

Sol–gel techniques are capable of producing a variety of SSA thin film materials with various selectivity and durability characteristics. The benefits of such surfaces are comparative simplicity in production and the potential for good cost-effectiveness. There are, nonetheless, many technical obstacles that need to be addressed before such techniques can become fully viable in the context of

commercial applications. Metal oxides and spinel-based absorbers are easy to synthesize using sol–gel methods but most of their selectivities are relatively lower than the commercial absorber surfaces. More explorations on precursor′s combinations, absorber stack configuration and compositions as well as the application of superior antireflection layer are needed to improve their selectivities. Metal particles embedded in matrix-type absorbers are among the better selective absorbers, but there are still problems associated with the reproducibility of the sol and few studies have been done on this type of absorber using sol–gel methods. The use of highly soluble raw materials and the avoidance of compounds that easily settle in precursor′s preparation is the robust way to solve the reproducibility problem. Likewise, carbon particles integrated in various matrices have not been comprehensively explored for synthesis of SSAs and as such, more technical studies are still required. Additionally, other pertinent factors such as the thickness of silica (especially if used as a matrix), abrasion, corrosion resistance and the durability of the absorber should also be examined more extensively in future research. In terms of policy implications, sol–gel solar selective absorber materials can be promoted in the context of flat plate solar collectors as benchmarked with other selective absorber materials. In line with this, to further promote applications of flat plate solar selective absorber materials, policy instruments should include the following components: feed-in-tariff, investment tax credits, subsidies, renewable energy portfolio, financing facilitation, public investment, government mandates and regulatory provisions.

References

[1] Hernández-Moro J, Martínez-Duart JM. Analytical model for solar PV and CSP electricity costs: present LCOE values and their future evolution. Renew Sustain Energy Rev 2013;20:119–32.

[2] Tyagi VV, Kaushik SC, Tyagi SK. Advancement in solar photovoltaic/thermal (PV/T) hybrid collector technology. Renew Sustain Energy Rev 2012;16: 1383–98.

[3] Ibrahim A, Othman MY, Ruslan MH, Mat S, Sopian K. Recent advances in flat plate photovoltaic/thermal (PV/T) solar collectors. Renew Sustain Energy Rev 2011;15:352–65.

[4] Fang X, Li D. Solar photovoltaic and thermal technology and applications in China. Renew Sustain Energy Rev 2013;23:330–40.

[5] Kalogirou SA. Solar thermal collectors and applications. Prog Energy Combust Sci 2004;30:231–95.

[6] Kennedy CE. Review of mid- to high-temperature solar selective absorber materials. Technical report TP-520-31267. Golden, CO, USA: National Renewable Energy Laboratory; 2002

[7] Barrera E, Viveros T, Montoya A, Ruiz M. Titanium–tin oxide protective films on a black cobalt photothermal absorber. Solar Energy Mater Solar Cells 1999;57:127–40.

[8] Barshilia HC, Selvakumar N, Rajam KS, Sridhara Rao DV, Muraleedharan K. Deposition and characterization of $TiAlN/TiAlON/Si_3N_4$ tandem absorbers prepared using reactive direct current magnetron sputtering. Thin Solid Films 2008;516:6071–8.

[9] Oelhafen P, Schüler A. Nanostructured materials for solar energy conversion. Solar Energy 2005;79:110–21.

[10] Katumba G, Olumekor L, Forbes A, Makiwa G, Mwakikunga B, Lu J, et al. Optical, thermal and structural characteristics of carbon nanoparticles embedded in ZnO and NiO as selective solar absorbers. Solar Energy Mater Solar Cells 2008;92:1285–92.

[11] Konttinen P, Lund PD, Kilpi RJ. Mechanically manufactured selective solar absorber surfaces. Solar Energy Mater Solar Cells 2003;79:273–83.

[12] Ienei E, Isac L, Cazan C, Duta A. Characterization of $Al/Al_2O_3/NiO_x$ solar absorber obtained by spray pyrolysis. Solid State Sci 2010;12:1894–7.

[13] Crnjak Orel Z, Klanjšek Gunde M, Lenček A, Benz N. The preparation and testing of spectrally selective paints on different substrates for solar absorbers. Solar Energy 2000;69(Supplement 6):131–5.

[14] Tabor H. Selective radiation. I. Wavelength discrimination: a new approach to the harnessing of solar energy. Bull Res Council Isr 1956;5A:119–28.

[15] Tabor H. Selective radiation. II. Wavefront discrimination: a new approach to the harnessing of solar energy. Bull Res Council Isr 1956;5A:129–34.

[16] Tabor H. Transactions of the conference on the use of solar energy, vol. 11. Section A1-23. Tucson: University of Arizona Press; 1956.

[17] Zemanová M, Chovancová M, Gáliková Z, Krivošík P. Nickel electrolytic colouring of anodic alumina for selective solar absorbing films. Renew Energy 2008;33:2303–10.

[18] Wazwaz A, Salmi J, Bes R. The effects of nickel-pigmented aluminum oxide selective coating over aluminum alloy on the optical properties and thermal efficiency of the selective absorber prepared by alternate and reverse periodic plating technique. Energy Convers Manag 2010;51:1679–83.

[19] Hutchins MG, Wright PJ, Grebenik PD. Comparison of different forms of black cobalt selective solar absorber surfaces. Solar Energy Mater 1987;16:113–31.

[20] Xiao X, Miao L, Xu G, Lu L, Su Z, Wang N, et al. A facile process to prepare copper oxide thin films as solar selective absorbers. Appl. Surf. Sci. 2011;257:10729–36.

[21] Selvakumar N, Barshilia HC, Rajam KS, Biswas A. Structure, optical properties and thermal stability of pulsed sputter deposited high temperature $HfO_x/Mo/HfO_2$ solar selective absorbers. Solar Energy Mater Solar Cells 2010;94: 1412–20.

[22] Wäckelgård E, Hultmark G. Industrially sputtered solar absorber surface. Solar Energy Mater Solar Cells 1998;54:165–70.

[23] Toshiro M. Copper oxide thin films prepared by chemical vapor deposition from copper dipivaloylmethanate. Solar Energy Mater Solar Cells 1998;56:85–92.

[24] Kaluza L, Orel B, Drazic G, Kohl M. Sol–gel derived $CuCoMnO_x$ spinel coatings for solar absorbers: structural and optical properties. Solar Energy Mater Solar Cells 2001;70:187–201.

[25] Barrera E, Avila A, Mena J, Lara VH, Ruiz M, Méndez-Vivar J. Synthesis of cobalt–silicon oxide thin films. Solar Energy Mater Solar Cells 2003;76: 387–98.

[26] Bostrom T, Wackelgard E, Westin G. Solution-chemical derived nickel–alumina coatings for thermal solar absorbers. Solar Energy 2003;74: 497–503.

[27] Japelj B, Vuk AŠ, Orel B, Perše LS, Jerman I, Kovač J. Preparation of a TiMEMO nanocomposite by the sol–gel method and its application in coloured thickness insensitive spectrally selective (TISS) coatings. Solar Energy Mater Solar Cells 2008;92:1149–61.

[28] Bayón R, San Vicente G, Maffiotte C, Morales Á. Preparation of selective absorbers based on CuMn spinels by dip-coating method. Renew Energy 2008;33:348–53.

[29] Juang R-C, Yeh Y-C, Chang B-H, Chen W-C, Chung T-W. Preparation of solar selective absorbing coatings by magnetron sputtering from a single stainless steel target. Thin Solid Films 2010;518:5501–4.

[30] Adsten M, Joerger R, Järrendahl K, Wäckelgård E. Optical characterization of industrially sputtered nickel–nickel oxide solar selective surface. Solar Energy 2000;68:325–8.

[31] Zhao S, Ribbing C-G, Wäckelgård E. Optical constants of sputtered Ni/NiO solar absorber film—depth-profiled characterization. Solar Energy Mater Solar Cells 2004;84:193–203.

[32] Zhao S, Wäckelgård E. Optimization of solar absorbing three-layer coatings. Solar Energy Mater Solar Cells 2006;90:243–61.

[33] Vince J, Šurca Vuk A, Krašovec UO, Orel B, Kohl M, Heck M. Solar absorber coatings based on CoCuMnOx spinels prepared via the sol–gel process: structural and optical properties. Solar Energy Mater Solar Cells 2003;79:313–30.

[34] Zhao S, Wäckelgård E. The optical properties of sputtered composite of Al–AlN. Solar Energy Mater Solar Cells 2006;90:1861–74.

[35] Yin Y, Pan Y, Hang LX, McKenzie DR, Bilek MMM. Direct current reactive sputtering Cr–Cr2O3 cermet solar selective surfaces for solar hot water applications. Thin Solid Films 2009;517:1601–6.

[36] Nejati M. Cermet based solar selective absorbers: further selectivity improvement and developing new fabrication technique: Saarländische Universitäts und Landesbibliothek; 2008.

[37] Harizanov OA, Gesheva KA, Stefchev PL. Sol–gel and CVD-metal oxide coatings for solar energy utilization. Ceram Int 1996;22:91–4.

[38] Voinea M, Bogatu C, Chitanu GC, Duta A. Copper cermets used as selective coatings for flat plate solar collectors. Rev Chim (Bucuresti) 2008;59:659–63.

[39] Kanu SS, Binions R. Thin films for solar control applications. Proc R Soc A: Math Phys Eng Sci 2010;466:19–44.

[40] Konttinen P, Lund PD. Microstructural optimization and extended durability studies of low-cost rough graphite–aluminum solar absorber surfaces. Renew Energy 2004;29:823–39.

[41] Bostrom T, Valizadeh S, Lu J, Jensen J, Westin G, Wäckelgård E. Structure and morphology of nickel–alumina/silica solar thermal selective absorbers. J Non-Crystal Solids 2011;357:1370–5.

[42] Bayon R, San Vicente G, Morales A. Durability tests and up-scaling of selective absorbers based on copper–manganese oxide deposited by dipcoating. Solar Energy Mater Solar Cells 2010;94:998–1004.

[43] Bostrom T, Westin G, Wäckelgård E. Optimization of a solution-chemically derived solar absorbing spectrally selective surface. Solar Energy Mater Solar Cells 2007;91:38–43.

[44] Barrera E, Huerta L, Muhl S, Avila A. Synthesis of black cobalt and tin oxide films by the sol–gel process: surface and optical properties. Solar Energy Mater Solar Cells 2005;88:179–86.

[45] Katumba G, Lu J, Olumekor L, Westin G, Wäckelgård E. Low cost selective solar absorber coatings: characteristics of carbon-in-silica synthesized with sol–gel technique. J Sol–Gel Sci Technol 2005;36:33–43.

[46] Rincón ME, Molina JD, Sánchez M, Arancibia C, García E. Optical characterization of tandem absorber/reflector systems based on titanium oxide–carbon coatings. Solar Energy Mater Solar Cells 2007;91:1421–5.

[47] Brinker CJ, Frye GC, Hurd AJ, Ashley CS. Fundamentals of sol–gel dip coating. Thin Solid Films 1991;201:97–108.

[48] Kozelj M, Vuk AS, Jerman I, Orel B. Corrosion protection of Sunselect, a spectrally selective solar absorber coating, by (3-mercaptopropyl)trimethoxysilane. Solar Energy Mater Solar Cells 2009;93:1733–42.

[49] Jerman I, Koželj M, Orel B. The effect of polyhedral oligomeric silsesquioxane dispersant and low surface energy additives on spectrally selective paint coatings with self-cleaning properties. Solar Energy Mater Solar Cells 2010;94:232–45.

[50] Kaluza L, Šurca-Vuk A, Orel B, Dražič G, Pelicon P. Structural and IR spectroscopic analysis of sol–gel processed CuFeMnO$_4$ spinel and CuFeMnO$_4$/silica films for solar absorbers. J Sol–Gel Sci Technol 2001;20:61–83.

[51] Bostrom TK, Wackelgard E, Westin G. Anti-reflection coatings for solution-chemically derived nickel–alumina solar absorbers. Solar Energy Mater Solar Cells 2004;84:183–91.

[52] Klanjšek Gunde M, Kožar Logar J, Crnjak Orel Z, Orel B. Optimum thickness determination to maximise the spectral selectivity of black pigmented coatings for solar collectors. Thin Solid Films 1996;277:185–91.

[53] Duffie JA, Beckman WA. Solar engineering of thermal processes. third ed. New Jersey: John Wiley & Sons Inc; 2006.

[54] Uma C, Malhotra L, Chopra K. Cobalt oxide–iron oxide selective coatings for high temperature applications. Bull Mater Sci 1986;8:385–9.

[55] Farooq M, Lee ZH. Computations of the optical properties of metal/insulator-composites for solar selective absorbers. Renew Energy 2003;28:1421–31.

[56] Cathro KJ. Preparation of cobalt-oxide-based selective surfaces by a dip-coating process. Solar Energy Mater 1984;9:433–47.

[57] Mastai Y, Polarz S, Antonietti M. Silica–carbon nanocomposites—a new concept for the design of solar absorbers. Adv Funct Mater 2002;12:197–202.

[58] Bayón R, Vicente GS, Maffiotte C, Morales Á. Development of solar absorbers based on spinel-type materials deposited by dip-coating. Solar PACES 2006.

[59] Barrera-Calva E, Mendez-Vivar J, Ortega-Lopez M, Huerta-Arcos L, Morales-Corona J, Olayo-Gonzalez R. Silica–copper oxide composite thin films as solar selective coatings prepared by dipping sol–gel. Res Lett Mater Sci 2008;2008:1–5.

[60] Karlsson T, Roos A. Optical properties and spectral selectivity of copper oxide on stainless steel. Solar Energy Mater 1984;10:105–19.

[61] Hottel HC, Unger TA. The properties of a copper oxide—aluminum selective black surface absorber of solar energy. Solar Energy 1959;3:10–5.

[62] Márquez A, Blanco G, Fernandez de Rapp ME, Lamas DG, Tarulla R. Properties of cupric oxide coatings prepared by cathodic arc deposition. Surf Coat Technol 2004;187:154–60.

[63] Scherer A, Inal OT, Singh AJ. Investigation of copper oxide coatings for solar selective applications. Solar Energy Mater 1983;9:139–58.

[64] Scherer A, Inal OT, Pettit RB. Modelling of degradation in black copper photothermal collector coatings. J. Mater. Sci. 1988;23:1923–33.

[65] Sathiaraj TS. Solar selective properties of copper–aluminum composite films. Indian J Pure Appl Phys 2007;45:613–7.

[66] Gillette RB. Selectively emissive materials for solar heat absorbers. Solar Energy 1960;4:24–32.

[67] Barrera EC, Viveros TG, Morales U. Preparation of selective surfaces of black cobalt by the sol–gel process. Renew Energy 1996;9:733–6.

[68] Maruyama T, Nakai T. Cobalt oxide thin films prepared by chemical vapor deposition from cobalt (II) acetate. Solar Energy Mater 1991;23:25–9.

[69] Choudhury C, Sehgal HK. Black cobalt selective coatings by spray pyrolysis for photothermal conversion of solar energy. Solar Energy 1982;28:25–31.

[70] Choudhury C, Sehgal HK. High temperature degradation in cobalt oxide selective absorber. Solar Energy 1983;30:291–2.

[71] Chidambaram K, Malhotra LK, Chopra KL. Spray-pyrolysed cobalt black as a high temperature selective absorber. Thin Solid Films 1982;87:365–71.

[72] Avila GA, Barrera CE, Huerta AL, Muhl S. Cobalt oxide films for solar selective surfaces, obtained by spray pyrolisis. Solar Energy Mater Solar Cells 2004;82:269–78.

[73] Barrera E, Viveros T, Avila A, Quintana P, Morales M, Batina N. Cobalt oxide films grown by a dipping sol–gel process. Thin Solid Films 1999;346:138–44.

[74] Drasovean R, Monteiro R, Fortunato E, Musat V. Optical properties of cobalt oxide films by a dipping sol–gel process. J Non-Crystal Solids 2006;352:1479–85.

[75] Goyal DJ, Agashe CM, Marathe BR, Takwale MG, Bhide VG. Effect of precursor solution concentration on the structural properties of sprayed ZnO films. J Mater Sci Lett 1992;11:708–10.

[76] John S, Nagarani N, Rajendran S. Black cobalt solar absorber coatings. Solar Energy Mater 1991;22:293–302.

[77] Barrera E, González I, Viveros T. A new cobalt oxide electrodeposit bath for solar absorbers. Solar Energy Mater Solar Cells 1998;51:69–82.

[78] Kadirgan F, Sohmen M. Development of black cobalt selective absorber on copper for solar collectors. Turk J Chem 1999;23:345–51.

[79] Brown-Shaklee HJ, Carty W, Edwards DD. Spectral selectivity of composite enamel coatings on 321 stainless steel. Solar Energy Mater Solar Cells 2009;93:1404–10.

[80] Crnjak Orel Z, Orel B, Klanjšek Gunde M. Spectrally selective SnO_2: film on glass and black enamelled steel substrates: spray pyrolytical deposition and optical properties. Solar Energy Mater Solar Cells 1992;26:105–16.

[81] Simonis F, Faber AJ, Hoogendoorn CJ. Porcelain enamelled absorbers, coated by spectral selective tin oxide. J Solar Energy Eng 1987;109:22–5.

[82] Rizzato AP, Broussous L, Santilli CV, Pulcinelli SH, Craievich AF. Structure of SnO_2 alcosols and films prepared by sol–gel dip coating. J Non-Crystal Solids 2001;284:61–7.

[83] Barrera CE, Avila GA, Rodil S, Huerta L. Cobalt–copper oxide compound for selective solar absorber. In: World renewable energy congress (WREC) VIII 2004.

[84] Morales-Ortiz U, Avila-García A, Hugo Lara CV. Ruthenium oxide films for selective coatings. Solar Energy Mater Solar Cells 2006;90:832–40.

[85] Qian W, Xu-dong C, Hui W, Tao M. Study on preparation and properties of NiO–Al$_2$O$_3$ solar selective absorption films. Surf Technol 2011;40:1.

[86] Dudita M, Isac L, Duta A. Influence of solvents on properties of solar selective coatings obtained by spray pyrolysis. Bull Mater Sci 2012;35:997–1002.

[87] Voinea M, Ienei E, Bogatu C, Duta A. Solar selective coatings based on nickel oxide obtained via spray pyrolysis. J Nanosci Nanotechnol 2009;9:4279–84.

[88] Niklasson GA, Granqvist CG. Surfaces for selective absorption of solar energy: an annotated bibliography 1955–1981. J Mater Sci 1983;18:3475–534.

[89] Lu YM, Hwang WS, Yang JS, Chuang HC. Properties of nickel oxide thin films deposited by RF reactive magnetron sputtering. Thin Solid Films 2002;420 and 421:54–61.

[90] He Z, Ji Z, Zhao S, Wang C, Liu K, Ye Z. Characterization and electrochromic properties of Cu$_x$Ni$_{1-x}$O films prepared by sol–gel dip-coating. Solar Energy 2006;80:226–30.

[91] Bostrom TK, Wackelgard E, Westin G. Durability tests of solution-chemically derived spectrally selective absorbers. Solar Energy Mater Solar Cells 2005;89:197–207.

[92] Nejati MR, Fathollahi V, Khalaji Asadi M. Computer simulation of the optical properties of high-temperature cermet solar selective coatings. Solar Energy 2005;78:235–41.

[93] Niklasson GA, Granqvist CG, Hunderi O. Effective medium models for the optical properties of inhomogeneous materials. Appl. Opt. 1981;20:26–30.

[94] Niklasson G. Optical properties and solar selectivity of coevaporated Co–Al$_2$O$_3$ composite films. J Appl Phys 1984;55:3382.

[95] Voinea M, Vladuta C, Bogatu C, Duta A. Surface properties of copper based cermet materials. Mater Sci Eng: B 2008;152:76–80.

[96] Eisenhammer T, Schellinger H, Lazarov M. Process for producing selective absorbers. US patent. United States 1999.

[97] Bostrom TK, Wäckelgård E. Optical properties of solution-chemically derived thin film Ni–Al2O3 composites and Si, Al and Si–Ti oxides. J Phys: Condens Matter 2006;18:7737.

[98] Bostrom T. Solution-chemically derived spectrally selective solar absorbers: with system perspectives on solar heating. Uppsala: Acta Universitatis Upsaliensis; 2006.

[99] Bostrom T, Jensen J, Valizadeh S, Westin G, Wäckelgård E. ERDA of Ni–Al$_2$O$_3$/SiO$_2$ solar thermal selective absorbers. Solar Energy Mater Solar Cells. 2008;92:1177–82.

[100] Wang X, Li H, Yu X, Shi X, Liu J. High-performance solution-processed plasmonic Ni nanochain–Al2O3 selective solar thermal absorbers. Appl. Phys. Lett. 2012;101:203109.

[101] Khamlich S, Nemraoui O, Mongwaketsi N, McCrindle R, Cingo N, Maaza M. Black Cr/α-Cr2O3 nanoparticles based solar absorbers. Phys B: Condens Matter 2012;407:1509–12.

[102] Etherden N, Tesfamichael T, Niklasson GA, Wackelgard E. A theoretical feasibility study of pigments for thickness-sensitive spectrally selective paints. J Phys D: Appl Phys 2004;37:1115–22.

[103] Katzen D, Levy E, Mastai Y. Thin films of silica–carbon nanocomposites for selective solar absorbers. Appl Surf Sci 2005;248:514–7.

[104] Charlot A, Bruguier O, Toquer G, Grandjean A, Deschanels X. Nanocomposites derived from silica and carbon for low temperature photothermal conversion. Thin Solid Films 2014;553:157–60.

[105] Liu Z, Jin Z, Li W, Qiu J. Preparation of ZnO porous thin films by sol–gel method using PEG template. Mater Lett 2005;59:3620–5.

[106] Roro K, Tile N, Yalisi B, De Gama M, Wittes T, Roberts T, et al. Selective solar absorber coating research at the CSIR (South Africa); 2011.

[107] Roro KT, Tile N, Forbes A. Preparation and characterization of carbon/nickel oxide nanocomposite coatings for solar absorber applications. Appl Surf Sci 2012;258:7174–80.

[108] Roro KT, Tile N, Mwakikunga B, Yalisi B, Forbes A. Solar absorption and thermal emission properties of multiwall carbon nanotube/nickel oxide nanocomposite thin films synthesized by sol–gel process. Mater Sci Eng: B 2012;177:581–7.

[109] Hallenstvet M., Tilset B.G., Denkmann V., Siemen A., Lacau A., Simon C., et al. Method for making an absorber coating for solar heating, the coating as such and its application. US Patent 20,130,064,981; 2013.

[110] Geng Q-F, Zhao X, Gao X-H, Liu G. Sol–gel combustion-derived CoCuMnO$_x$ spinels as pigment for spectrally selective paints. J Am Ceram Soc 2011;94:827–32.

[111] Bayón R, San Vicente G, Maffiotte C, Morales Á. Characterization of copper–manganese–oxide thin films deposited by dip-coating. Solar Energy Mater Solar Cells 2008;92:1211–6.

[112] Carlsson B, Frei U, Kohl M, Moller K. Accelerated life testing of solar energy materials—case study of some selective solar absorber coating materials for DHW Systems. Solar Materials Research and Development—Solar Heating and Cooling Program: Report of Task X. Borås, Sweden: International Energy Agency; 1994.

[113] Carlsson B, Frei U, Kohl M, Moller K, Brunold S. Qualification test procedure for solar absorber surface durability. Solar Energy Mater Solar Cells 2000;61:255–75.

[114] Amri A, Duan X, Yin C-Y, Jiang Z-T, Rahman MM, Pryor T. Solar absorptance of copper–cobalt oxide thin film coatings with nano-size, grain-like morphology: optimization and synchrotron radiation XPS studies. Appl Surf Sci 2013;275:127–35.

[115] Amri A, Jiang Z-T, Zhao X, Xie Z, Yin C-Y, Ali N, et al. Tailoring the physicochemical and mechanical properties of optical copper–cobalt oxide thin films through annealing treatment. Surface Coat Technol 2014;239: 212–21.

[116] Amri A, Zhong-Tao Jiang, Parisa A. Bahri, Chun-Yang Yin, Xiaoli Zhao, Zonghan Xie, et al. Surface electronic structure and mechanical characteristics of coppercobalt oxide thin film coatings: soft X-ray synchrotron radiation spectroscopic analyses and modeling. J Phys Chem C 2013;117:16457–67.

[117] Amri A, Jiang Z-T, Pryor T, Yin C-Y, Xie Z, Mondinos N. Optical and mechanical characterization of novel cobalt-based metal oxide thin films synthesized using sol–gel dip-coating method. Surface Coat Technol 2012;207:367–74.

[118] Xu Y, Zhang B, Hao Fan W, Wu D, Han Sun Y. Sol–gel broadband antireflective single-layer silica films with high laser damage threshold. Thin Solid Films. 2003;440:180–3.

[119] Chen D. Anti-reflection (AR) coatings made by sol–gel processes: a review. Solar Energy Mater Solar Cells 2001;68:313–36.

[120] Raut HK, Ganesh VA, Nair AS, Ramakrishna S. Anti-reflective coatings: a critical, in-depth review. Energy Environ Sci 2011;4:3779–804.

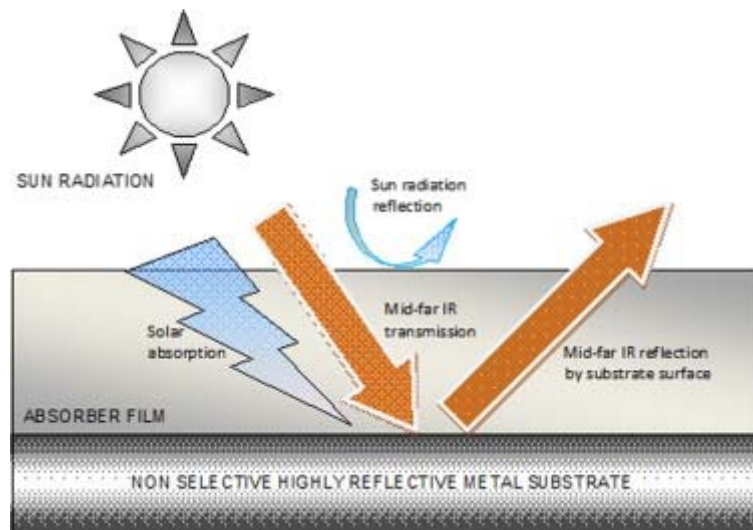Fig. 1. Solar selective absorption in the absorber–reflector tandem system.

Fig. 2. Spectral performance of an ideal and real selective solar absorber as well as the sun spectrum at AM1.5 and the blackbody-like emission spectra at different temperatures (adapted from ISO 9845-1:1992 and [10]).
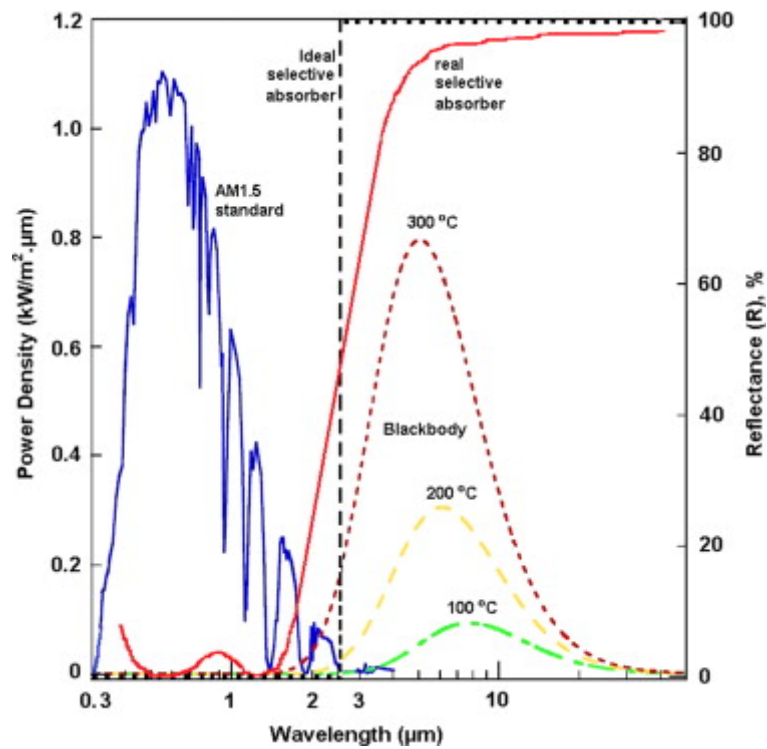
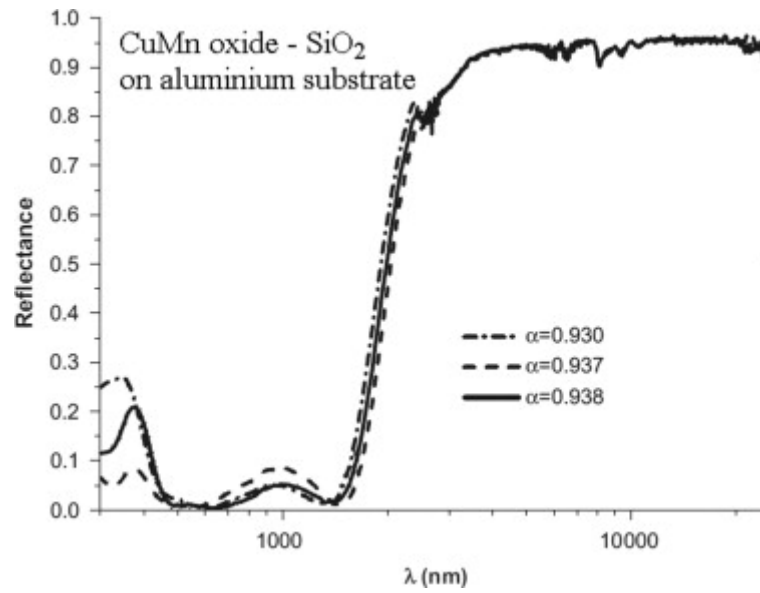Fig. 3. Reflectance spectra of CuMn oxide selective absorber (adapted from [28]).

Fig. 4. General strategy for synthesizing metal oxide/spinels (route A) and metal/carbon particles embedded in non-organic matrix/binder (route B) solar selective absorbers.
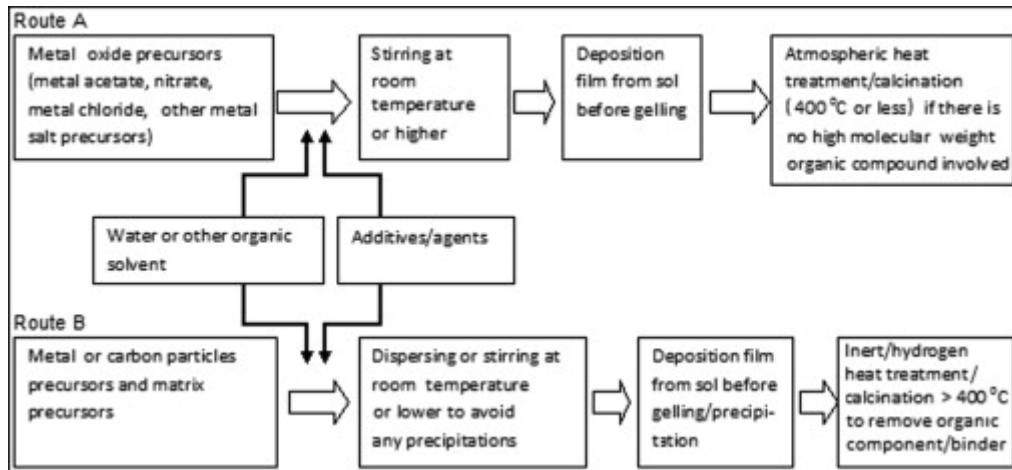
Table 1. Instruments and measurements ranges, reflectance types and air masses (AM) used in the absorptance and emittance characterizations of various SSAs produced by sol–gel methods.

SSA materials and substrates	Instruments and the measurements range		Reflectance type	Air mass (AM)	Reference
	Absorptance	Emittance			
$CuMnO_x$ on aluminum	UV–vis–NIR Perkin–Elmer LAMBDA 950 spectrophotometer (0.3–2.5 μm)	NICOLET NEXUS MAGNA IR spectrophotometer (2.5–25 μm)	Hemispherical reflectance	1.5	[28]
Cobalt oxide on stainless steel	Varian Cary 5E spectrophotometer (0.2–2.5 μm)	Nicolet 470 FTIR (2.5–25 μm)	Near normal reflectance	2	[72]
$NiO–Al_2O_3$ on aluminum	Lambda 25 Perkin–Elmer spectrophotometer. (0.25–2.5 μm)	Spectrum BX, Perkin–Elmer (2.5–20 μm)	–	–	[12]
Black cobalt on stainless steel	Varian 5E spectrophotometer. (0.2–2.5 μm)	Emissiometer	–	–	[67]
CoCuO on stainless steel	Varian Cary 5E spectrophotometer (0.2–2.5 μm)	Nicolet 470 FTIR spectrophotometer (2.5–25 μm)	–	–	[83]
RuO_2 on titanium	670 Thermo Nicolet FT spectrometer (UV–vis–NIR–MIR)		Near normal reflectance	2	[84]
Cobalt based oxide on stainless steel	Beckman DK2 spectrophotometer (0.3–2.5 μm)	Land surface thermometer and Gier–Dunkle DB100 infrared reflectometer	Total hemispherical reflectance	2	[56]
Cermet Ni–Al_2O_3 on aluminum	Perkin–Elmer Lambda 9 double beam (0.3–2.5 μm)	Bomen Michelson 110 FTIR (2.5–20 μm)	Normal reflectance		[51]
$C–SiO_2$ on glass	Jasco VERY-570 spectrophotometer (0.2–2 μm)	Emissiometer (EL 510–520 ELAN INFORMATIQUE)	Diffuse reflectance,		[99]
$C–SiO_2$ on Al and SS	Perkin–Elmer Lambda 900 double beam (0.3–2.5 μm)	Single beam FTIR Bomem–Michelson 110 spectr. (2.5–20 μm)	Near normal hemispherical reflectance		[45]
C–NiO	Perkin–Elmer Lambda 900 spectr. (0.3–2.5 μm)	Bomem DA8 Fourier transform and Bruker Tensor 27 spectr. (2.5–20.0 μm)	Near-normal reflectance		[10]
$C–TiO_2$ on stainless steel	Shimadzu UV-3101 PC spectrophotometer (0.25–2.5 μm)	Bruker FTIR-5000 spectr. (2.5–22 μm)	Normal reflectance		[46]
$CuFeMnO_4$ black film spinel	Fourier-transform spectr. Bruker IFS 66 with a PTFE coated integrating sphere (measurements in range <2.3 μm)	Fourier-transform spectr. Bruker IFS 66 with a diffuse gold coated sphere (> 1.7 μm)	Near-normal hemispherical reflectance (0.3–17 μm)	1.5	[50]
Black cobalt–tin oxide on SS and glass	Varian Cary 5E spectrophotometer (0.2–2.5 μm)	Nicolet 750 FTIR (2.5–25 μm)	Near normal reflectance		[44]

Table 2. Summary of absorptance (α) and emittance (ε) of various SSA materials produced by sol–gel methods.

Sol–gels SSA materials and substrates	α	ε	Reference
Metal oxide based absorber			
Bare CuO on aluminum	0.93	0.11 (80 °C)	[61]
CuO–SiO$_2$ on stainless steel	0.92	0.2	[59]
Black cobalt on galvanized iron	0.91	0.12 (100 °C)	[69]
Cobalt oxide on stainless steel	0.93	0.14 (100 °C)	[71]
CoFeO on stainless steel	0.94	0.20 (100 °C)	[54]
Cobalt oxide on stainless steel	0.77	0.2	[72]
Cobalt oxide–nickel oxide on mild steel	0.9	0.10 (80 °C)	[56]
Black cobalt on stainless steel	0.88	0.12	[67]
Black cobalt–tin oxide on nickel stainless steel	0.72	0.04 (100 °C)	[44]
Cobalt oxide-copper oxide on stainless steel	0.84	0.28	[83]
Ruthenium oxide on the ASTM grade 2titanium	0.74	0.12	[84]
Nickel oxide–alumina on aluminum	0.92	0.03	[12]
Cermet based absorber			
Nickel–alumina cermet on aluminum	0.97	0.05	[43]
Carbon–silica on glass	0.94	0.15	[99]
Carbon–NiO on aluminum	0.84	0.04	[10]
Carbon–ZnO on aluminum	0.71	0.06	[10]
Ni nanochain–alumina on stainless steel	>0.9	<0.1	[100]
MWCNTs in NiO on aluminum	0.84	0.2 (100 °C)	[108]
Spinels based absorber			
CuCoMnO$_x$ on aluminum	0.9	0.05	[24]
CuCoMnO$_x$–SiO$_x$ on aluminium	0.91	0.04	[33]
CuMn oxide–SiO$_2$ on aluminium	0.95	0.06 (100 °C)	[42]
Cu$_x$Co$_y$O$_z$ on aluminium	0.83	–	[114]